Bull Volcanol (2008) 70:547–562
DOI 10.1007/s00445-007-0153-2

RESEARCH ARTICLE

Sumisu volcano, Izu-Bonin arc, Japan: site of a silicic caldera-forming eruption from a small open-ocean island

Kenichiro Tani · Richard S. Fiske · Yoshihiko Tamura · Yukari Kido · Jiro Naka · Hiroshi Shukuno · Rika Takeuchi

Received: 30 January 2006 / Accepted: 16 April 2007 / Published online: 28 June 2007

Abstract Sumisu volcano was the site of an eruption during 30–60 ka that introduced ~48–50 km^3 of rhyolite tephra into the open-ocean environment at the front of the Izu-Bonin arc. The resulting caldera is 8×10 km in diameter, has steep inner walls 550–780 m high, and a floor averaging 900 m below sea level. In the course of five research cruises to the Sumisu area, a manned submersible, two ROVs, a Deep-Tow camera sled, and dredge samples were used to study the caldera and surrounding areas. These studies were augmented by newly acquired single-channel seismic profiles and multi-beam seafloor swath-mapping. Caldera-wall traverses show that pre-caldera eruptions built a complex of overlapping dacitic and basaltic edifices, that eventually grew above sea level to form an island about 200 m high. The caldera-forming eruption began on the island and probably produced a large eruption column. We interpret that prodigious rates of tephra fallback overwhelmed the Sumisu area, forming huge rafts of floating pumice, choking the nearby water column with hyperconcentrations of slowly settling tephra, and generating pyroclastic gravity currents of water-saturated pumice that traveled downslope along the sea floor. Thick, compositionally similar pumice deposits encountered in ODP Leg 126 cores 70 km to the south could have been deposited by these gravity currents. The caldera-rim, presently at ocean depths of 100–400 m, is mantled by an extensive layer of coarse dense lithic clasts, but syn-caldera pumice deposits are only thin and locally preserved. The paucity of syn-caldera pumice could be due to the combined effects of proximal non-deposition and later erosion by strong ocean currents. Post-caldera edifice instability resulted in the collapse of a 15° sector of the eastern caldera rim and the formation of bathymetrically conspicuous wavy slump structures that disturb much of the volcano's surface.

Keywords Submarine caldera · Silicic volcanism · Caldera-forming eruption · Tephra dispersal · Late Pleistocene eruption · Edifice instability · Izu-Bonin arc

Editorial responsibility: J. McPhie

K. Tani (✉) · Y. Tamura · Y. Kido · J. Naka · H. Shukuno
Institute for Frontier Research on Earth Evolution (IFREE), Japan Agency for Marine-Earth Science and Technology (JAMSTEC),
2-15 Natsushima-cho,
Yokosuka 237-0061, Japan
e-mail: kentani@jamstec.go.jp

R. S. Fiske
Smithsonian Institution MRC-119,
Washington, DC 20013-7012, USA

R. Takeuchi
Department of Earth and Planetary Science, University of Tokyo,
Tokyo 113, Japan

Introduction

The Izu-Bonin arc extends from Hakone volcano on the Japanese island of Honshu to the Ogasawara Islands, 1,000 km to the south (Fig. 1). A chain of volcanic islands, extending from Izu-Oshima to Aogashima, is located along the northern half of the arc. Farther south, islands are less common and smaller, and the volcanic front is defined by a series of submarine caldera volcanoes.

We here describe and interpret the Sumisu volcano, the largest of these southern submarine caldera volcanoes and where ~48–50 km^3 of rhyolite tephra was erupted during 30–60 ka. We describe the geological development of the caldera area and interpret the caldera-forming eruption, particularly the ways in which large volumes of pumiceous tephra were dispersed in the open-ocean, arc-front environment. We

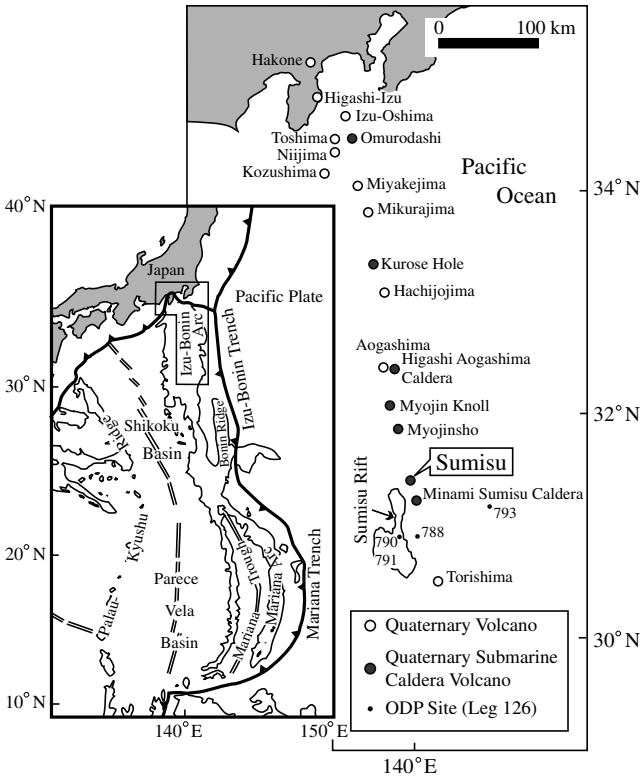

Fig. 1 Map showing location of Sumisu volcano and other seafloor features south of Japan

examine the possibility that Sumisu eruptions may have been the source of the thick pumice deposits encountered during ODP Leg 126 seafloor drilling, 70 km to the south and southeast.

The present research, plus the small number of similar studies in today's oceans (e.g. Carey et al. 2000; Fiske et al. 2001; Smith et al. 2003; Wright et al. 2003, 2006) are steps toward better understanding of large-scale, submarine silicic volcanism. Collectively, these studies complement those of similar volcanism on land, which has commanded much attention over the past several decades. In addition, studies of present-day seafloor silicic calderas will permit better interpretation of submarine caldera-forming eruptions and their products in ancient terrains, where deformation and metamorphism commonly mask original textures and structures. The association of economically important volcanic-hosted massive sulfide deposits with these volcanic centers (e.g. Gibson et al. 1999; Hudak et al. 2003; Mueller et al. 1994) underscores the need to know more about silicic submarine volcanism.

Previous Sumisu related studies

Recent bathymetric studies along the front of the Izu-Bonin arc have identified seven submarine caldera volcanoes between the islands of Izu-Oshima and Torishima (Murakami and Ishihara 1985; Nagaoka et al. 1991; Yuasa et al. 1991). Volcanological studies in the Sumisu area, using manned submersibles, remote operating vehicles (ROVs), camera sleds (Deep-Tow), and dredging, began in the 1980s in conjunction with the seafloor drilling projects of ODP Leg 126. (e.g. Taylor et al. 1990; Klaus et al. 1992). Iwabuchi (1999) carried out the first manned submersible investigations in the Sumisu area, and the present study builds on his pioneering work. Detailed petrological and geochemical studies of the Sumisu volcano have been presented by Tamura et al. (2005) and Shukuno et al. (2006).

The name *Sumisu* has interesting origins (S. Oshima, written communication, 2004). The first recorded Western contact with Sumisu took place in 1851, when the crew of an American sailing ship, captained by a Mr. Smith, discovered a 136-m-high sea stack and named it Smith Island (Fig. 2). The Japanese retained the name Smith but transliterated it to Sumisu, the name still in use today.

Field and analytical methods

Fieldwork was carried out during five cruises operated by the Japan Agency for Marine-Earth Science and Technology (JAMSTEC). Locations of our surveys, the equipment used, and shipboard operations are presented in Fig. 3 and Tables 1 and 2. Fieldwork utilizing a manned submersible, ROVs and a Deep-Tow camera sled differs in important ways from studies on land. The illumination for reliable observation is limited, and dives last for only a few hours. In addition, it is difficult to linger at an outcrop for detailed observations, because ROVs and Deep-Tows are tethered to moving ships. Instability of submersibles and ROVs can make detailed, in situ sampling difficult, especially on steep cliffs. On the contrary, these limitations are offset by the

Fig. 2 Eastern wall of Sumisu Island; its summit is 136 m high

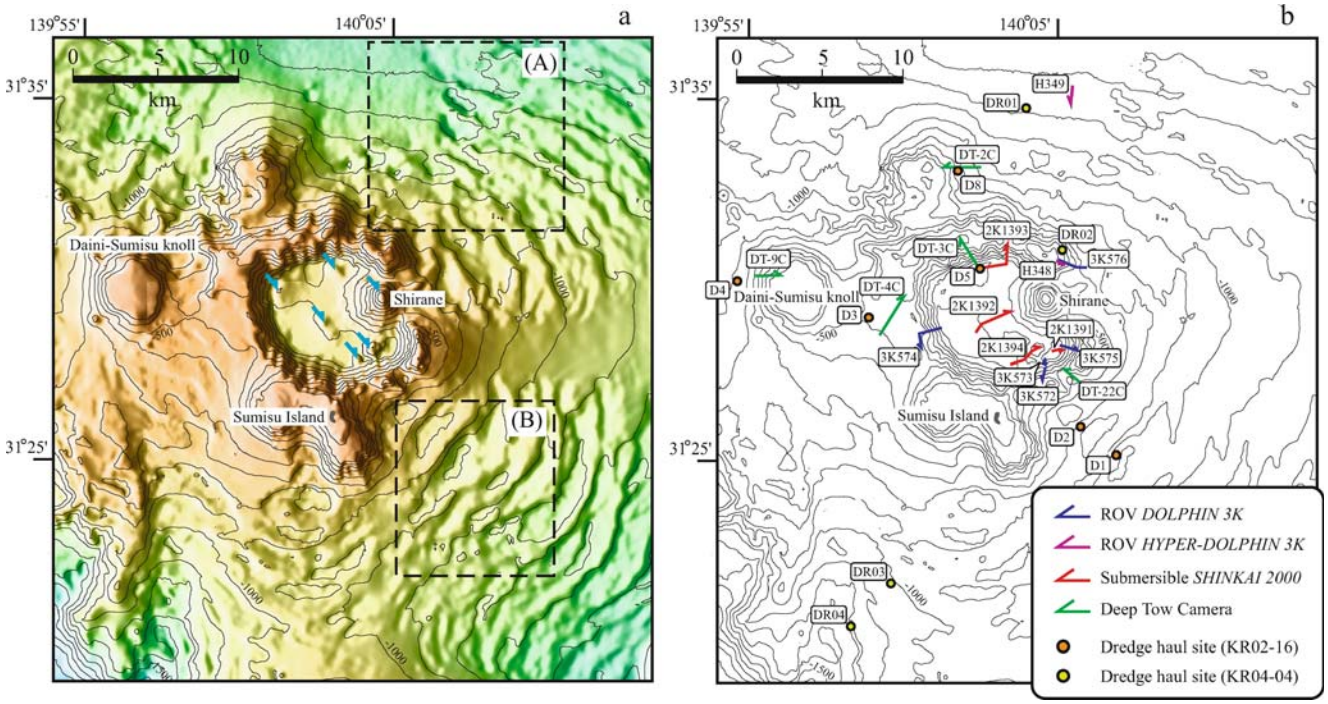

Fig. 3 Bathymetry of Sumisu volcano, contour interval 100 m. **a** Proximal areas dominated by the caldera and the wavy slump structures that disturb the volcano's surface. *Blue arrows* point to post-caldera cones. *Dashed squares* (*A*) and (*B*) outline areas shown in Fig. 10. Bathymetric color-key shown in Fig. 4. **b** Sampling and dive-track locations

ability to investigate caldera walls from floor to rim. Many modern subaerial calderas are filled with lakes, limiting access to complete caldera-wall sections and post-caldera features.

Single-channel seismic (SCS) surveys employed a 350 in.^{3} GI-gun with shot intervals of 6.9 and 8.0 s. Onboard data processing was done using PRO-MAX and SPW (PARALLEL GEOSCIENCES, Inc., U.S.A.). Bathymetric data were obtained with the multi-beam seafloor swath-mapping systems (SEABEAM2112/SEABAT8160) aboard JAMSTEC's research vessels.

X-ray fluorescence (XRF) analyses of samples were performed at Institute for Frontier Research on Earth Evolution (IFREE), JAMSTEC, using RIGAKU SIMLTEX

Table 1 Cruise data in the Sumisu area

Cruise no.	Surveyed area	Employed systems	Operations
NT02-16 (Sept. 20–Oct. 11, 2002)			
R/V *NATSUSHIMA*	Sumisu caldera	ROV *DOLPHIN 3K*, submersible *SHINKAI 2000*	Rock sampling, geological observation
KR02-16 (Dec. 10–Dec. 27, 2002)			
R/V *KAIREI*	Sumisu caldera, Daini-Sumisu knoll, Minami Sumisu caldera		Dredge hauls, single-channel seismic survey, multi-narrow beam bathymetric survey
KY03-10 (Sept. 4–Sept. 20, 2003)			
R/V *KAIYO*	Sumisu caldera, Daini-Sumisu knoll	4,000 m-class Deep-Tow camera	Geological observation, multi-channel seismic survey, multi-narrow beam bathymetric survey
KR04-04 (Apr. 15–Apr. 30, 2004)			
R/V *KAIREI*	Sumisu caldera, Minami Sumisu caldera		Dredge hauls, Single-channel seismic survey, multi-narrow beam bathymetric survey
NT04-10 (Sept. 6–Sept. 22, 2004)			
R/V *NATSUSHIMA*	Sumisu caldera, Daiichi- and Daini-Sumisu knoll	ROV *HYPER-DOLPHIN*	Rock sampling, geological observation, multi-narrow beam bathymetric survey

Table 2 Data relating to submersible/ROV dives, dredge hauls, Deep-Tow camera traverses

Dive/Dredge/Deep Tow No.	Area studied/operations
3K572	Base to middle of the southeastern wall of Sumisu caldera/geological observation, sampling
3K573	Middle to top of the southeastern wall of Sumisu caldera/geological observation, sampling
3K574	Base to top of western wall of Sumisu caldera/geological observation, sampling
3K575	Base to top of southeastern wall of Sumisu caldera/geological observation, sampling
3K576	Slope of northeastern Sumisu edifice/geological observation, sampling
2K1391	Southeast floor of Sumisu caldera/geological observation, sampling
2K1392	Central to northeastern floor of Sumisu caldera/geological observation, sampling
2K1393	Northern floor and base of northern wall of Sumisu caldera/geological observation, sampling
2K1394	Center cones on the southeastern Sumisu caldera floor/geological observation, sampling
D1	Wavy slump, slope of southeastern Sumisu edifice/dredge haul
D2	Wavy slump, slope of southeastern Sumisu edifice/dredge haul
D3	Top of western Sumisu edifice/dredge haul
D4	Western foothill of Daini-Sumisu knoll/dredge haul
D5	Northern wall of Sumisu caldera/dredge haul
D8	Eastern slope of small knoll, north of Sumisu caldera/dredge haul
DT-2C	Eastern slope of small knoll, north of Sumisu caldera/geological observation
DT-3C	Base to the top of northern wall of Sumisu caldera/geological observation
DT-4C	Top of western Sumisu edifice/geological observation
DT-9C	Eastern slope of Daini-Sumisu knoll/geological observation
DT-22C	Base to the top of southeastern wall of Sumisu caldera/geological observation
DR01	Slope of northeastern Sumisu edifice/dredge haul
DR02	Slope of northern Sumisu edifice/dredge haul
DR03	Wavy slump, slope of southwestern Sumisu edifice/dredge haul
DR04	Wavy slump, slope of southwestern Sumisu edifice/dredge haul
DR06	Southern slope of Minami Sumisu caldera/dredge haul
H348	Slope of northeastern Sumisu edifice/geological observation, sampling
H349	Slope of northern Sumisu edifice/geological observation, sampling

3K ROV *DOLPHIN 3K*, *2K* manned submersible *SHINKAI 2000*, *D* dredge haul on RV Kairei cruise KR02-16, *DT* Deep-Tow camera traverse, *DR* dredge on RV Kairei cruise KR04-04, *H* ROV *HYPER-DOLPHIN*

12 for major elements and RIGAKU RIX3000 for trace elements. Analytical methods and conditions are described in Tani et al. (2005). Brine contamination was removed by repeatedly boiling samples in distilled water. Major elements were analyzed on 11-times diluted glass beads, and trace elements were analyzed on pressed pellets. The relative standard deviation (RSD) of the repeated analyses is <0.71% for major elements and <7.2% for trace elements.

Carbon and oxygen isotopes were measured to interpret the origin of carbonate that locally cements caldera-rim pumice and lithic clasts. The analyses were carried out at the Department of Earth and Planetary Science, University of Tokyo. The sample preparation methods and isotope measurement techniques are based on Morishita and Matsuhisa (1984). The carbonate samples were rinsed with distilled water and acetone and later dissolved in phosphate to produce CO_2 gas. The CO_2 gas was then analyzed by a Finnigan MAT252 mass spectrometer to determine $^{13}C/^{12}C$ and $^{18}O/^{16}O$ ratios. The data were standardized by PDB and VSMOW. The analytical precision of the delta values is less than ±0.13‰ for both carbon and oxygen isotopes.

Geology of Sumisu volcano

We define Sumisu volcano as the crudely elliptical cluster of submarine volcanoes centered at 31°30′N on the front of the Izu-Bonin arc (Fig. 4). Using the 1,000 m bathymetric contour to define its outline, the volcano measures about 40×25 km along E–W and N–S directions, respectively. A nearly unbroken slope to the east extends to the floor of the Izu-Ogasawara trench at ocean depths >9,000 m; the North Sumisu rift basin cuts deeply into the western flank of Sumisu volcano.

Bathymetric knolls, representing the summits of volcanoes that coalesced to form the complex, dot Sumisu volcano's surface. The most conspicuous of these, Daini-Sumisu knoll, lies about 6 km west of Sumisu caldera (Fig. 3), and others are roughly clustered along E–W directions. The clustered growth of these small- and medium-size basaltic to silicic volcanoes could have been the precursor to larger-scale magmatism that led to caldera-forming eruptions, as has been interpreted at numerous other volcanic complexes, both subaerial and submarine

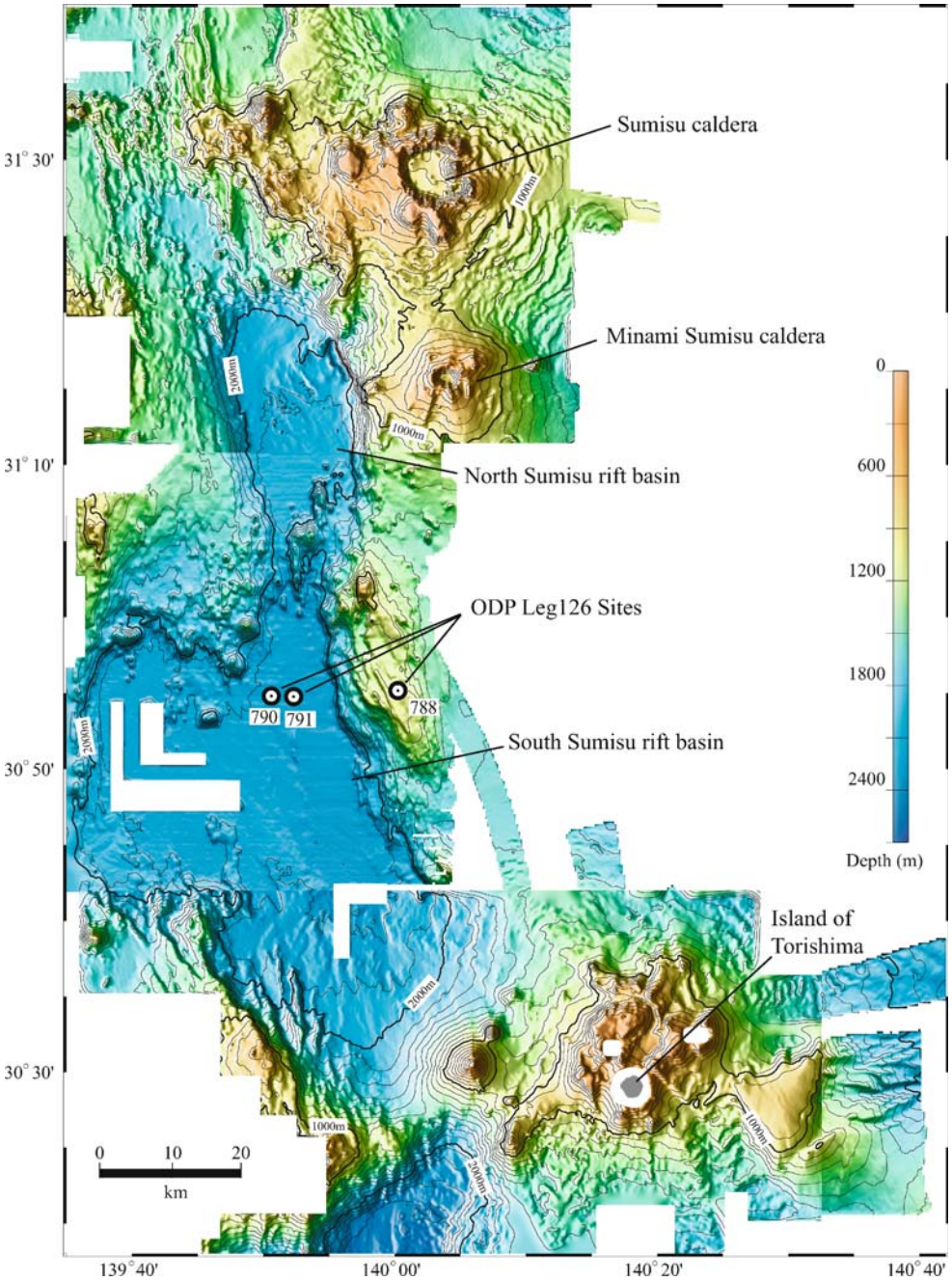

Fig. 4 Bathymetric map of the Sumisu–Torishima area; contour interval 100 m

(e.g. the Crater Lake caldera in Oregon, U.S.A.; Bacon 1983; Bacon and Lanphere 2006, and the submarine Myojin Knoll volcano, 40 km north of Sumisu; Fiske et al. 2001). This interpretation is strengthened by ROV and Deep-Tow observations of Sumisu's caldera walls, where cross sections of coalesced volcanoes are exposed.

Sumisu Island

The 136-m-high sea stack of Sumisu Island (Fig. 2) is made of reddened and oxidized basalt lavas, scoria, and associated intrusions. Beds dip irregularly a few degrees to the south, supporting the notion that the present-day feature is a remnant of a larger, pre-caldera island, the summit of which once lay somewhere to the north. Extrapolation of Sumisu's present-day submarine slopes suggests that the summit of this island was about 200 m above sea level.

Caldera-wall geology

ROV observations (Fig. 5) show that dacitic and basaltic coherent facies (lava flows and intrusions) and associated breccias make up the lower 30–40% of caldera-wall

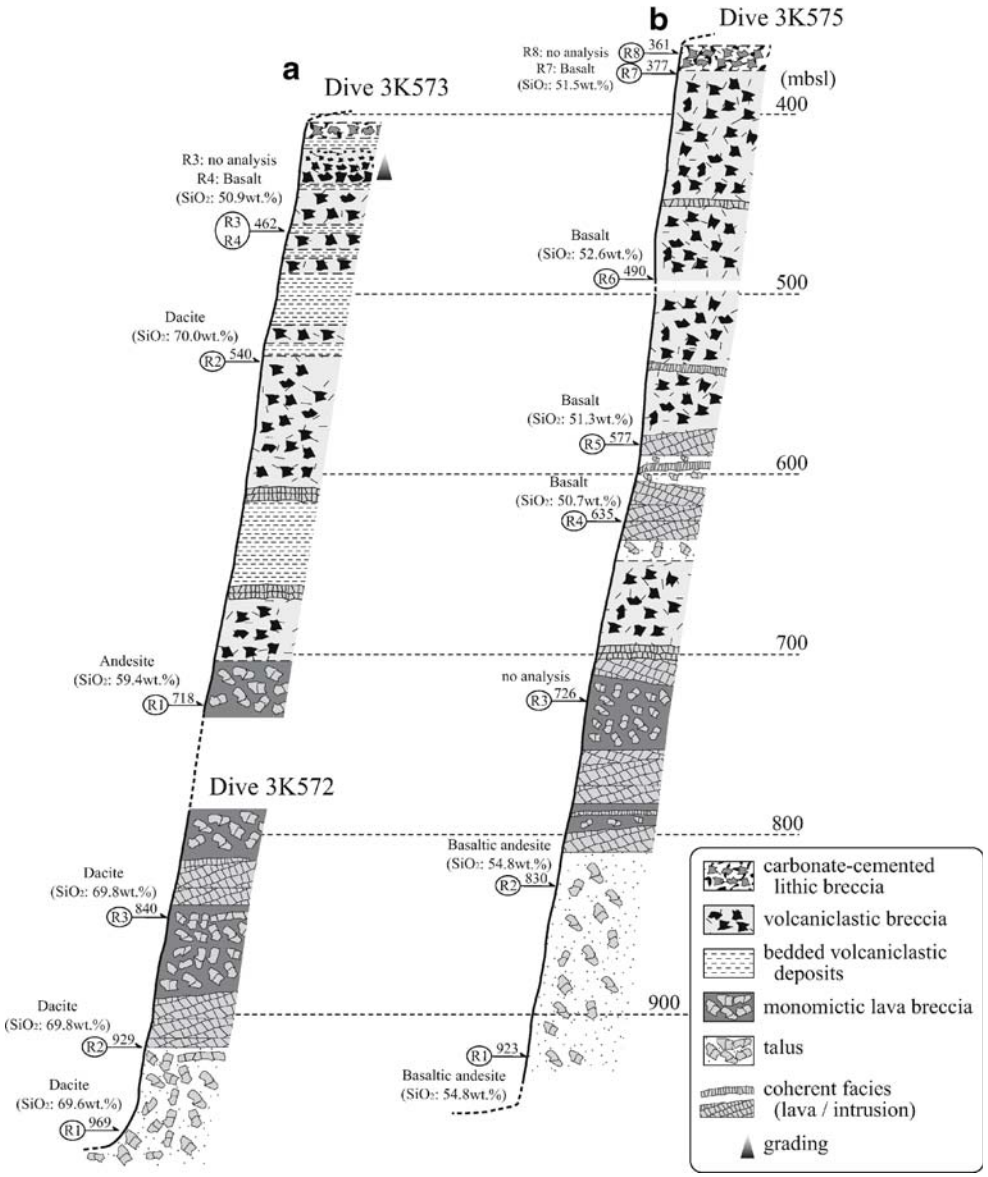

Fig. 5 Sumisu caldera-wall sections from ROV traverses; lithologies in covered intervals are interpreted. *Numbered dashed lines* and *number on arrows* showing sampling point indicate ocean depth in meters below sea level (mbsl).
a Southern wall.
b Southeastern wall

sections. These units are overlain by a wide variety of gently dipping volcaniclastic deposits. Steeply dipping dikes cut all of these units. The dikes are distinguished from the lava flows by the presence of chilled margins and/or zones of sub-horizontal cooling joints. Overall, caldera-wall physiography consists of a series of steep cliffs separated by talus-covered shelves. Selected major and trace element data of caldera-wall samples are presented in Table 3.

Massive dacitic coherent units (Fig. 6a) and coarse monomictic breccias make up the bulk of the lower 100–200 m of the southern caldera wall (Fig. 5a, Dive 3K572 and 3K573). The traverse up the southeastern caldera wall encountered a small basaltic volcano, made up of lavas and dikes that is nested between the dacitic volcanoes that make up most of the pre-caldera edifice (Fig. 5b, Dive 3K575). The bathymetric knoll, seen on the southeastern caldera rim and rising to a depth of 200 m, may be the summit of this basaltic volcano. Two clasts of orthopyroxene-bearing basaltic andesite were collected from talus at the base of the southeastern wall, but outcrops of these rocks were not found.

Upper parts of the southern caldera wall are dominated by buff colored, gently dipping pumiceous volcaniclastic deposits that in general are finer grained than the monomictic breccias below. These units first appear at depths of about 650–550 m and continue intermittently to the top of the caldera wall (Fig. 6b). Bed thicknesses range from a few cm

Table 3 Major and trace-element data for selected samples from the Sumisu–Torishima area

Sample	3K575-R4	2K1391-R3	2K1393-R8	2K1394-R3	3K576-R1	3K576-R3	3K576-R5	3K576-R7	DR01-01	DR01-R06	DR06-R03	DR06-R08
Rock	Caldera wall basalt	Caldera wall andesite	Caldera wall dacite	Caldera floor dome dacite	Syn-caldera pumice	Syn-caldera pumice	Syn-caldera pumice	Syn-caldera pumice	Syn-caldera pumice	Syn-caldera pumice	Minami Sumisu pumice	Minami Sumisu pumice
(wt%)												
SiO_2	49.8	55.8	67.8	68.0	71.1	71.3	72.7	72.4	73.3	73.1	70.3	74.4
TiO_2	0.49	0.65	0.69	0.74	0.46	0.47	0.43	0.42	0.43	0.42	0.37	0.32
Al_2O_3	16.1	16.5	14.8	14.5	12.7	12.8	12.8	12.7	13.0	12.8	14.9	13.3
Fe_2O_3	9.43	9.06	5.26	5.50	4.97	5.04	4.85	4.75	4.93	4.83	4.81	1.99
MnO	0.15	0.16	0.14	0.19	0.15	0.15	0.15	0.15	0.15	0.15	0.17	0.10
MgO	8.35	4.87	1.61	1.25	0.40	0.44	0.40	0.40	0.55	0.41	0.56	0.40
CaO	12.6	9.82	4.53	4.61	2.93	3.05	2.90	2.85	2.93	2.88	2.90	2.55
Na_2O	2.17	2.61	3.56	4.28	4.39	4.34	4.51	4.51	4.60	4.57	5.35	4.31
K_2O	0.04	0.36	1.15	0.60	0.88	0.91	0.90	0.91	0.89	0.92	1.10	1.19
P_2O_5	0.05	0.10	0.16	0.19	0.10	0.11	0.10	0.09	0.10	0.10	0.10	0.07
Total	99.2	99.9	99.7	99.8	98.1	98.6	99.7	99.2	100.8	100.2	100.5	98.6
FeO*/MgO	1.02	1.67	2.94	3.97	11.1	10.3	10.95	10.8	8.08	10.6	8.54	5.04
(ppm)												
Ba	55.0	79.2	186.3	151.2	224.7	209.7	232.3	225.3	236.1	231.6	166.2	257.0
Ni	81.2	23.4	6.4	7.1	8.4	10.3	9.6	6.8	–	–	3.8	–
Cu	109.0	78.1	3.2	–	15.3	13.9	11.6	10.9	13.0	11.9	–	6.1
Zn	64.5	72.3	82.6	101.0	101.9	101.7	102.0	99.5	93.1	89.5	62.1	41.3
Pb	–	3.3	4.9	3.4	4.7	4.5	6.5	5.0	7.6	6.5	2.7	5.6
Th	–	–	0.7	–	1.0	0.8	0.9	0.7	1.1	–	1.0	0.8
Rb	0.5	5.2	14.6	8.0	13.2	12.9	13.8	13.6	13.8	14.6	14.7	19.9
Sr	136.3	160.5	176.6	202.4	143.3	146.7	143.0	141.6	143.5	141.4	205.7	133.3
Y	12.1	20.6	37.1	39.4	49.3	49.1	50.1	50.1	50.6	49.6	39.3	30.3
Zr	20.6	52.4	110.4	91.4	127.0	125.8	130.4	131.6	132.8	129.6	162.6	127.4
Nb	0.4	0.6	1.0	0.9	1.0	1.2	1.0	1.0	1.1	1.2	1.9	1.2
Zr/Y	1.7	2.6	3.0	2.3	2.6	2.6	2.6	2.6	2.6	2.6	4.1	4.2
(vol.%)												
ol	2.05	–	–	–		–	–	–	–	–	–	–
pl	24.7	18.6	8.4	6.2		0.6	tr.	–	tr.	tr.	6.2	–
cpx	11.3	6.0	0.6	0.8		tr.	–	–	–	–	0.2	–
opx	–	2.5	0.3	0.4		tr.	–	–	tr.	tr.	2.1	–
opq	–	–	0.7	0.7		tr.	tr.	–	tr.	tr.	0.9	tr.
gm	61.9	72.9	90.1	91.8		99.4	100.0	100.0	100.0	100.0	90.6	100.0
Total	100.0	100.0	100.0	100.0		100.0	100.0	100.0	100.0	100.0	100.0	100.0

*FeO** total iron recalculated as FeO., *ol* olivine, *pl* plagioclase, *cpx* clinopyroxene, *opx* orthopyroxene, *opq* opaque mineral, *gm* groundmass, *tr*: trace

to >5 m. The thick units (>5 m) are massive and consist mostly of fine breccia; these units contain scarce angular to subangular dark lithic clasts, most <20 cm in diameter. The thinner beds range in thickness from about a few centimeters to about 1 m and locally display low-angle truncations and channels. Cross beds were not observed. Several bedded intervals contain local concentrations of dark 10–20 cm subangular lithic clasts. We infer that these upper-caldera-wall deposits consist mostly of resedimented volcaniclastic debris, although some may have been direct products of eruptions.

Syn-caldera pumice and associated deposits

Perhaps the most noteworthy feature of Sumisu volcano's geology is the paucity of proximal pumice genetically related to its caldera-forming eruption. Thin (2–5 m) deposits of angular, fresh, and pale-buff rhyolite pumice occur only locally at the top of the caldera wall, but these are rare. Shukuno et al. (2006) found the caldera wall to be composed of rocks ranging from basalt to rhyolite (<70.0 wt% SiO_2). In contrast, rhyolitic pumice samples collected from the few syn-caldera deposits found differ

Fig. 6 Facies exposed in Sumisu caldera wall. **a** Massive dacitic coherent unit; southern caldera wall, 840 mbsl. **b** Thinly bedded volcaniclastic deposits; southern caldera wall, 440 mbsl. **c** Fines-poor syn-caldera pumice deposit at top of western caldera wall, 330 mbsl. Widths of each view is uncertain but in the range 2 to 4 m

from those in the wall and have SiO_2 >71.0 wt% (Table 3). These deposits are unconsolidated or only slightly consolidated, and none are welded or sintered. The pumice clasts, most <25 cm in diameter, are highly vesicular and phenocryst-poor (<1 vol.%). The scarce phenocrysts are plagioclase, clinopyroxene, orthopyroxene, and titanomagnetite (Table 3).

The syn-caldera pumice deposits at Sumisu were found in situ at the following two places only:

1) ROV Dive 3K574 encountered a 3-4-m-thick massive, fines-poor pumice deposit capping the western caldera wall (Fig. 6c), but steep cliffs prevented sampling.
2) Deep-Tow camera traverse DT-03C found a similar, 2-m-thick fines-poor pumice deposit at the top of the northern caldera wall.

Syn-caldera pumice mantles an extensive area at and near the northeastern caldera rim, but we have no evidence that these accumulations are primary. Dive 3K576 encountered extensive pumice talus mantling the gentle outer slope of the Sumisu edifice from depths of 650 to 320 m. Dive H348 revisited the upper part of this same traverse and documented vaguely bedded, weakly cemented, pumice outcrops preserved in dozens of low, subparallel ribs (Fig. 7a). Accumulations of dense lithic blocks and lapilli were seen between some of the ribs. The long axes of these ribs are aligned along an azimuth of ~120°, the average orientation of the southeast-directed ocean currents that we infer to have carried away most of the pumice, leaving the subparallel ribs as erosional remnants. The vague internal beds (<30 cm) are parallel from rib to rib, suggesting that continuous pumice lapilli layers once capped the northeastern caldera rim.

A clast-supported veneer of angular coarse lithic clasts (most <50 cm in diameter) was observed to overlie the syn-caldera pumice deposits described at sites (1) and (2) above, as well as elsewhere over wide areas of the caldera rim (Fig. 7b). This veneer is the youngest caldera-wall unit found and consists of a wide variety of igneous rocks, including aphanitic to porphyritic basalt and dacite. We could estimate the thickness of this veneer only along the two traverses noted above, where it is 1–2 m thick. Elsewhere, its thickness is unknown, because it was observed from above (from ROVs and the Deep-Tow camera sled), and cross sections were not visible.

In places on the western, southern and southeastern caldera wall, this veneer of lithic clasts is cemented by calcite, forming a conspicuously rough-surfaced 1.5–2 m layer of what we informally call gasa-gasa [Japanese for *rough*]. Thin sections of the gasa-gasa show crystals of calcite cementing the subangular to angular lithic and

Fig. 7 Post-caldera features of Sumisu caldera. **a** Slightly cemented "rib-like" exposures of resedimented syn-caldera pumice deposit; northeastern caldera rim, 375 mbsl. View is ~4 m across. **b** Lithic-rich deposit mantles the southern caldera rim, 380 mbsl. View is ~3 m across. **c** Vertical view of dacitic lava dome; southern caldera floor, 895 mbsl; absence of sediment cover suggests young age. View is ~3 m across

pumice fragments that are <5 cm in diameter. About 80–90% of the fragments are angular basalt and dacite and the remainder is subangular rhyolitic pumice that may have been derived from the caldera-forming eruption.

The calcite cement was separated for detailed carbon and oxygen isotope study (Table 4). $\delta^{18}O_{PDB}$ of the calcite ranges from +3.19 to +3.81‰, and $\delta^{13}C_{PDB}$ ranges from +2.91 to +3.88‰. The $\delta^{18}O$ values fall in the range of +3.20 to +4.92 reported for the carbonate precipitated from seawater circulating in fissures and fractures within ultramafic rocks at ambient ocean-floor temperatures (Bonatti et al. 1980). We suggest that calcite cement is the product of non-hydrothermal seawater circulation that affected parts of the caldera rim.

Talus and caldera floor

Talus and tumbled blocks were observed on all caldera wall traverses and conceal 25–40% of caldera-wall sections (Fig. 5). More extensive talus occurs at the base of the wall, and we infer that such deposits surround the entire caldera floor. It is likely that the caldera walls were originally steeper than they are at present, but ongoing wasting is diminishing these slopes and increasing the rim-to-rim diameter of the caldera.

Most of the caldera floor is covered with pumiceous sand and pebbles, although lobes of coarser debris, likely the product of avalanches and grain flows from nearby caldera walls, were commonly observed. Dive 3K574 encountered subangular lava boulders >1 m in diameter that had rolled or skidded onto the floor and traveled for distances of a few hundred meters.

Caldera-floor volcanism

The floor of Sumisu caldera is dotted with post-caldera cones, providing evidence for post-caldera volcanism (Fig. 3a). The 800-m-high cone of Shirane is the youngest and most conspicuous, and its summit lies just 8 m below sea level. Dive 2K1392 visited the western base of Shirane and collected one subangular fragment of dacite (69.2 wt% SiO_2). Since Shirane is a relatively large structure (about 3 km in diameter), it is not certain whether this dacitic composition is representative of the entire Shirane composition. Given its substantial size, however, it is likely to be a polygenetic volcano.

Table 4 Carbon and oxygen isotope compositions of calcite that cement lithic clasts mantling the caldera rim (gasa-gasa)

	3K574-R8-1	3K574-R8-2	D8-R14	D4-R16
$\delta^{13}C/^{12}C_{(PDB)}$	3.88	3.81	2.91	2.98
$\delta^{18}O/^{16}O_{(PDB)}$	3.76	3.33	3.81	3.19

Two cones lie along the southern and southeastern margins of the caldera floor (Fig. 3a). Dive 2K1394 traversed these cones and revealed that they are small-volume extrusive lava domes the surfaces of which are free of sediment cover (Fig. 7c). These domes are mostly composed of dacites having two distinct compositions, 68.1–68.5 wt% SiO_2 (southern dome) and 69.1–69.2 wt% SiO_2 (southeastern dome).

Older knolls, 100–250 m high and completely mantled by pumiceous sand and pebbles, are also present and imply that caldera-floor eruptions have spanned a significant part of post-caldera time. Dive 2K1392 encountered one of these knolls near the center of the caldera. Others lie along the northwestern and northern caldera floor margins (Fig. 3a).

Seismic reflection profiles

Processed reflection profiles and the interpreted geology from two single-channel seismic (SCS) transects are shown in Fig. 8.

Poor reflections were obtained beneath Sumisu's knolls and caldera wall, probably because of steep slopes and the absence of suitable reflectors at depth. In contrast, volcaniclastic aprons bordering these features contain good reflectors and permit the following interpretations:

1) Seismically defined strata making up the western pre-caldera edifice of Sumisu volcano abut Daini-Sumisu knoll. The shape of this knoll and the lack of strong seismic reflections within it suggest it is a lava dome. This is supported by the Deep-Tow camera observation of Daini-Sumisu's western slope and its summit (Fig. 3b, DT-9C) that encountered abundant large (<3 m in diameter) angular to subangular pumice clasts mantling its surface.
2) Strata forming the apron east of Sumisu caldera (uncolored in A'–B') thicken dramatically toward the west, suggesting extensive deposition of volcaniclastics prior to the growth of Sumisu volcano.
3) The southern apron of the Sumisu complex overlaps, and is therefore younger, than the northern apron of Minami Sumisu volcano.

Discussion

Distal transport of Sumisu tephra: evidence from ODP cores

Nishimura et al. (1991, 1992) described rhyolite pumice layers as much as 118 m thick from ODP Leg 126 cores at

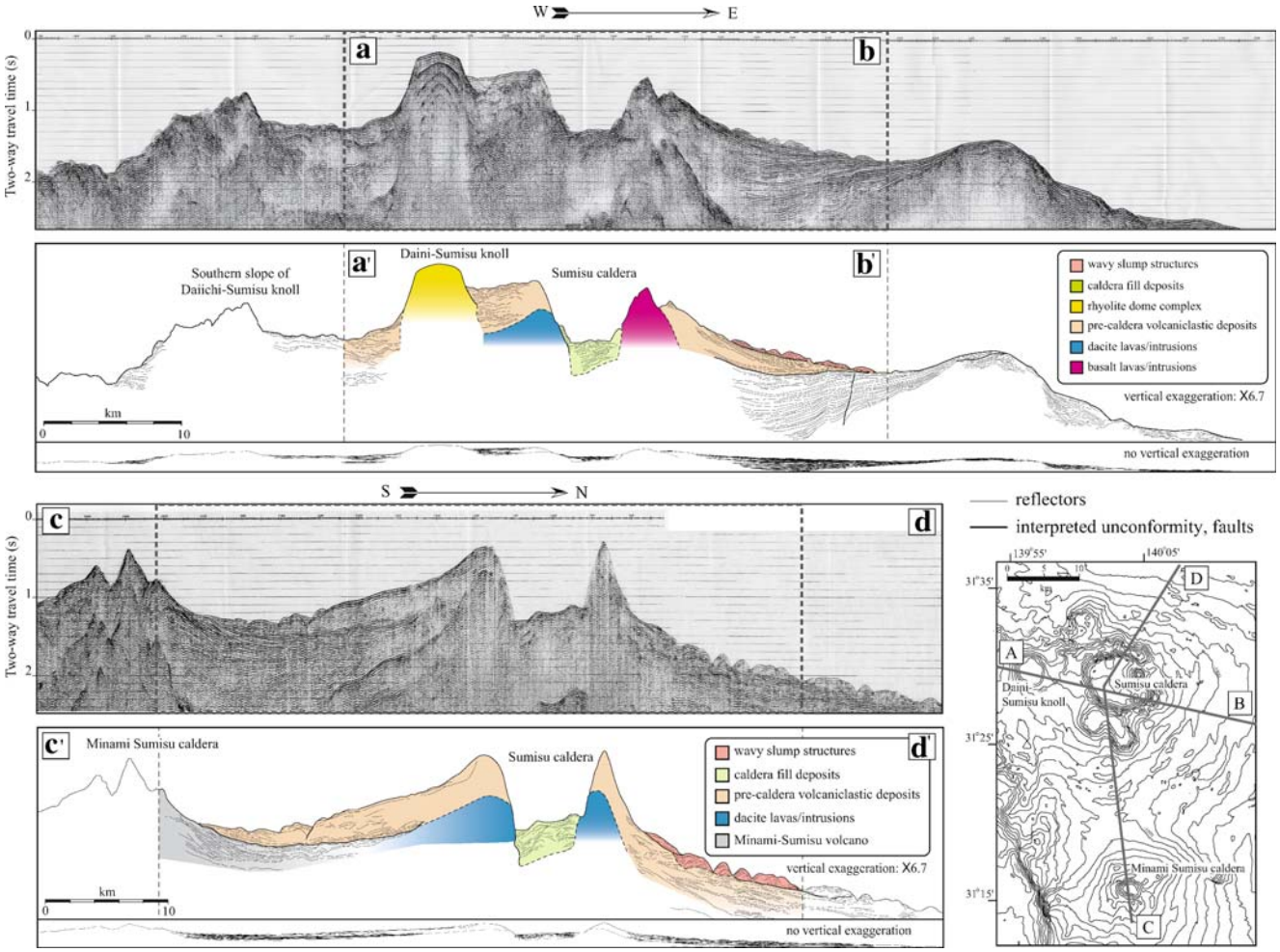

Fig. 8 Single-channel seismic profiles; ***a–b***, ***a'–b'*** and ***c–d***, ***c'–d'*** show raw data and interpreted geology, respectively. The deeper, repetitive reflections on ***a–b*** and ***c–d*** are multiple echoes and should be disregarded

Sites 790/791 (in the Sumisu rift), Site 788 (at the crest of the arc front), and Site 793 (on the eastern forearc slope). These sites lie about 70 km south and southeast of Sumisu (Fig. 1). Although these workers noted the unrestricted route for bottom-hugging gravity-current transport from Torishima volcano to the Sumisu rift sites, they favored Minami Sumisu caldera (Fig. 4) as the more likely source, because geochemical data then available suggested similarities of Minami Sumisu pumice clasts with those from the cores. These workers eliminated Sumisu caldera from consideration because a ridge of small knolls separating the northern and southern basins of the Sumisu rift was thought capable of blocking pumiceous gravity currents originating in the north. Klaus et al. (1992), however, presented bathymetry showing that the blocking ridge identified by Nishimura et al. (1992) actually contains a narrow channel through which pyroclastic gravity currents from Sumisu could have traveled to Sites 790/791.

Major- and trace-element data from Sumisu caldera, Minami Sumisu caldera and Torishima obtained by us and others since the early 1990s permit a reevaluation of pumice provenance (Table 3). A plot of SiO_2 versus K_2O (Fig. 9a) shows that the data from all nearby sources lie in the low-K field of Gill (1981). Most pumice samples from Minami Sumisu plot slightly higher than those from Sumisu, Torishima and the Leg 126 samples, but these data are not useful discriminators.

More useful is the incompatible element ratio (Zr/Y; Fig. 9b) which clearly distinguishes Minami Sumisu pumice samples from those obtained at other nearby sites. Minami Sumisu caldera, even though situated at the volcanic front, has geochemical characteristics different from those at the adjacent volcanic-front volcanoes, which, as noted by Hochstaedter et al. (2000), have Zr/Y ratios <2.5. Minami Sumisu caldera is therefore an unlikely source of the thick pumice layers at the ODP sites. The subordinate role of the Minami Sumisu as a source of voluminous seafloor pumice deposits is also implied by the fact that its caldera volume (~3.8 km^3) is about an order of magnitude less than that of the Sumisu caldera (~36 km^3).

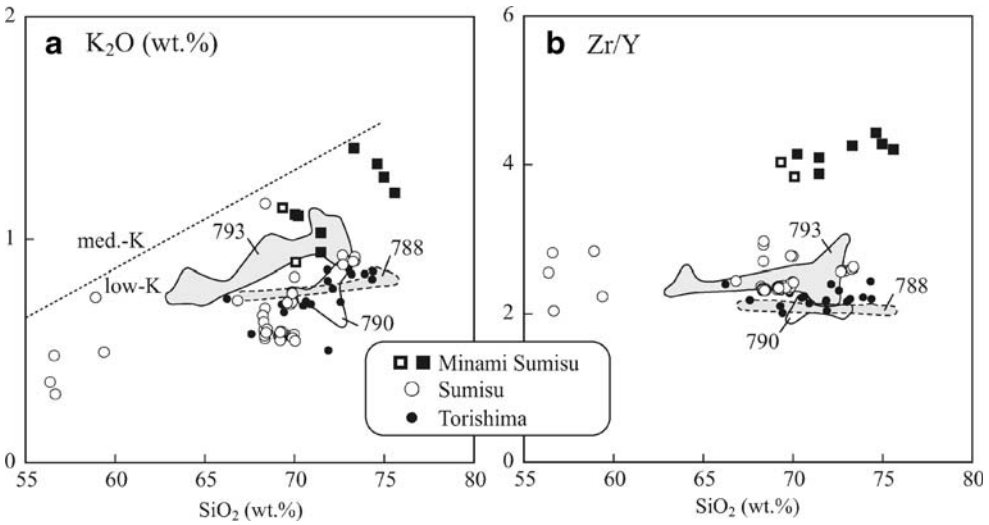

Fig. 9 **a** K_2O versus SiO_2 (wt%) diagram for silicic rocks (SiO_2 >55 wt%) in the Sumisu–Torishima area. *Open circles*, Sumisu caldera (this study); *solid squares*, Minami Sumisu caldera (this study); *open squares*, pumice samples from Minami Sumisu caldera (Yuasa and Nohara 1992); *solid circles*, submarine pumice samples from Torishima (K. Tani, unpublished data). The *numbered fields* show the range of Pleistocene pumice compositions collected at ODP Leg 126 sites 788, 790 and 793 (Gill et al. 1992). *Dashed line* separates the low-K and middle-K fields of Gill (1981). **b** Zr/Y versus SiO_2 (wt%) diagram of the same data shown in **a**

Discriminating between Sumisu and Torishima sources is more difficult. From available major and trace element data, pumice samples from both volcanoes are indistinguishable from each other, as well as from the Leg 126 pumice samples. Moreover, pumice samples from all of these sources have the identical phenocryst assemblage of clinopyroxene, orthopyroxene, plagioclase and titanomagnetite, the common assemblage in silicic rocks along the front of the Izu-Bonin arc (Tamura and Tatsumi 2002).

Our findings in the Torishima area, however, help to narrow the uncertainty (JAMSTEC unpublished cruise reports; KR02-16 and KY03-10). Only 4 of 12 dredge hauls near Torishima recovered mixtures of basalt, andesite and rhyolite pumice; the remaining 8 contained no pumice. Ten Deep-Tow camera traverses showed the sea floor surrounding Torishima to be underlain mainly by thick deposits of basalt scoria and coarser volcaniclastic debris, and newly acquired bathymetry shows no convincing evidence for the existence of a submarine caldera. Finally, outcrops on Torishima Island expose rocks ranging from basalt to dacite but no rhyolite.

We therefore conclude that Torishima was an unlikely source of the thick seafloor rhyolitic pumice deposits described by Nishimura et al. (1991, 1992) and infer that much of the thick seafloor pumice encountered at ODP Leg 126 Sites 790, 791, 788, and 793 was erupted from the Sumisu volcano. If true, large volumes of tephra from Sumisu's caldera-forming eruption traveled a minimum of 70 km to the south and southeast.

Caldera age

We found no direct evidence for the age of Sumisu caldera, but its youthfulness is suggested by the following:

1) The Sumisu magmatic system has fed recent eruptions and still emits heat. Iwabuchi (1999) discovered vent communities (including mussels and clams) clustered around warm (12.1°C) seeps near the summit of a caldera-floor cone. The two dacite domes discovered during this study (Dive 2K1394) are young features having no dusting of fine sediment (Fig. 7c). Small Sumisu-area eruptions are reported to have taken place in 1672, 1869, 1870, 1871, and 1873 (Siebert and Simkin 2002).
2) Caldera rim planation. Extensive parts of the northern and western caldera rim, lying at ocean depths of 140–300 m, have smooth, nearly-horizontal surfaces suggesting erosional planation during low stands of Pleistocene sea level. The maximum low sea-level stand occurred at about 18 ka (Chappell and Shackleton 1986), implying that the caldera rim (and thus the caldera itself) predates that event.
3) Correlations with dated ODP drill cores. Nishimura et al. (1991, 1992) used biostratigraphic- and sediment-accumulation-rate evidence from ODP drill cores in the Sumisu rift to suggest that thick pumiceous bed II and the combined III/IV beds at ODP sites 790/791 were deposited at 31 and 61 ka respectively. Based on the geochemical correlations discussed above, we

suggest that Sumisu's caldera-forming eruption took place during the late Pleistocene, sometime during 30–60 ka.

Edifice instability

Thin-skin slumping Concentric, wavy slump structures, although superficial, are conspicuous features of Sumisu bathymetry (Figs. 4 and 10) and deserve special attention. Keating et al. (2000) described similar features on submarine aprons flanking the volcanoes in Samoa and called them slump sheets. We prefer the informal term wavy slump structures, because of their map-view resemblance to waves formed by dropping a rock into a pond.

Detailed bathymetric maps of Sumisu's northeastern and southeastern slopes (Figs. 3a and 10) show these slump structures have crest-to-crest wave lengths of 1–3 km and frontal scarps 50–220 m high. The accompanying profiles show they traveled along 1°–7° slopes (Fig. 10). Many of these slump structures have bathymetrically defined depressions on their upper surfaces, and single channel seismic profiles show that the structures are 70–100 m thick; some display only slightly deformed internal bedding (Fig. 8). We interpret that the slumps resulted from the simultaneous slippage and associated rumpling of the uppermost, unlithified part of the Sumisu edifice. Offsets of bathymetric contours on the northeastern slope of the volcano (Fig. 10a) show that single slumps traveled 1–1.5 km downslope. Manned submersible observations along the upper southeastern slope of the Sumisu edifice (Iwabuchi 1999) showed the surface of these slumps to consist mostly of matrix-free jumbles of lithic clasts ranging in diameter from 10 cm to about 5 m.

The triggering mechanism for the wavy slump structures is unknown. Similar slumps disturb the slopes of Minami Sumisu volcano and the Torishima volcano complex, 25 and 85 km south of Sumisu, respectively, suggesting that these slumps share a common origin. In contrast, single channel seismic profiles across the Myojin Knoll and Myojinsho submarine volcanoes, respectively 80 and 60 km to the north, show the surfaces of these

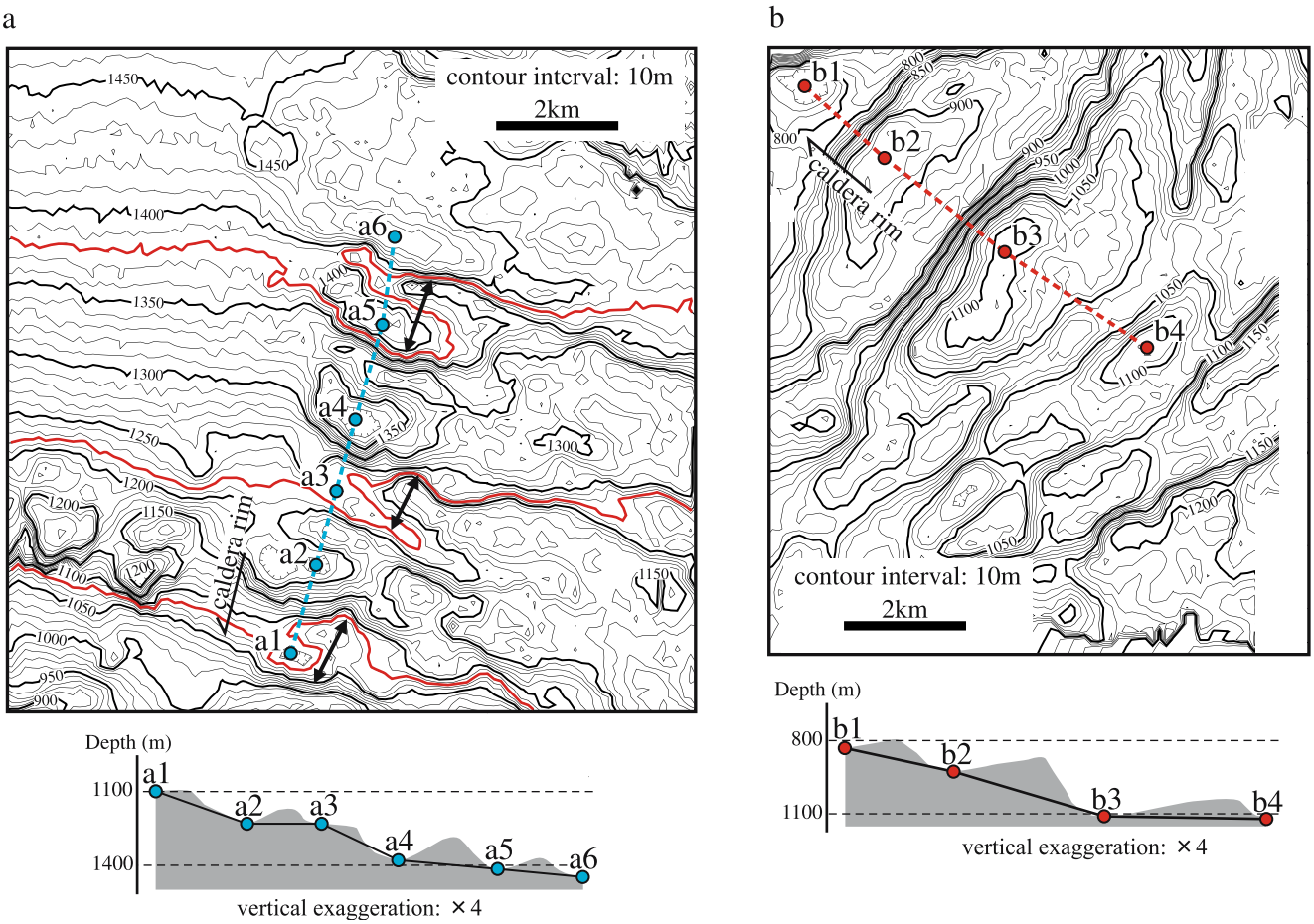

Fig. 10 Wavy slump structures; profiles show stair-step-like morphology. See Fig. 3a for index map. **a** Enlargement of northeastern slope; contour offsets suggest 1–1.5 km of downslope motion on 1°–7° slopes. **b** Enlargement of southeastern slope; profile shows slumps moved on 1°–4° slopes

edifices to be undisturbed. We favor the interpretation that one or more large tectonic earthquakes in the Sumisu–Torishima area triggered the wavy slump structures, one of the mechanisms suggested by Keating et al. (2000) for similar features in the Samoa area. Such earthquakes, common in the study area, are related to the nearby subduction beneath the Izu-Bonin trench. If true, the smooth-sloped Myojin Knoll and Myojinsho edifices to the north were sufficiently distant to have escaped the effects of these earthquakes.

Sector collapse A ~15° sector of the eastern caldera rim is missing as a result of small-scale collapse (Fig. 3). The post-caldera cone of Shirane partly fills the gap in the caldera rim that resulted from this collapse event.

Paucity of caldera-rim pumice deposits and abundance of lithic clasts

As noted above, only minor syn-caldera pumice deposits were found at or near Sumisu's caldera rim, whereas the same area is littered with lithic clasts. Assuming the pumice and the lithic clasts were both products of the caldera-forming eruption, how, and when, were these two fractions partitioned?

Proximal, syn-eruption partitioning Freundt (2003) conducted tank experiments in which heated mixtures of pumice and lithic clasts were allowed to flow into water. Although orders of magnitude smaller than the events during Sumisu's caldera-forming eruption, these experiments showed that dense clasts were deposited first and that less dense clasts traveled for greater distances. On a much larger scale, proximal deposition of dense lithic clasts also occurs during subaerial caldera-forming eruptions (e.g. Druitt and Sparks 1982; Walker 1985; Druitt and Bacon 1986).

Post-eruption erosion Strong ocean currents, common in the Sumisu area, could have preferentially eroded pumice clasts from the syn-caldera deposit, leaving dense lithic clasts behind. Dive H348 on the northeastern caldera rim encountered erosional remnants of a thin-bedded pumiceous sequence (Fig. 6d) that originally capped the northeastern caldera rim. Some of the pumice scoured from this area may be contained in the pumiceous scree that mantles the outer slopes of the Sumisu edifice just to the northeast (Dive 3K576).

We conclude that the scarcity of pumice and the high abundance of dense lithic clasts in proximal areas are likely to be the result of both syn-eruption preferential deposition of dense lithic clasts and post-eruption erosion of the more mobile pumice clasts, especially during the low stands of late Pleistocene sea level.

Volume of the caldera-forming eruption

Tephra deposits resulting from Sumisu's caldera-forming eruption are located entirely below sea level, so it is difficult to quantify their volume. However, by employing a template method to sum the volumes of the present-day caldera, the now-vanished pre-caldera island, and a 200-m-thick funnel-shaped mass to represent the volume of caldera fill, we estimate that about 36 km^3 of Sumisu's pre-caldera edifice was lost as a result of the caldera-forming eruption. At Crater Lake caldera, which has a slightly larger diameter than Sumisu caldera, Bacon (1983) estimated that ~9–12% of the pre-caldera edifice lost during the caldera-forming eruption has been enclosed as non-juvenile lithic clasts in the syn-caldera deposits. Assuming a similar percentage of non-juvenile lithic clasts in Sumisu, we therefore estimate that a volume of ~32–33 km^3 of Sumisu's pre-caldera edifice is missing. If the bulk density of the erupted juvenile tephra is two thirds that of the missing edifice, a tephra volume of ~48–50 km^3 is implied. As noted above, the multiple pumice layers encountered during nearby ODP drilling suggest that Sumisu may have been the site of repeated large-volume eruptions, but we here focus attention on the most recent event that we infer to be genetically related to the present caldera.

Caldera-forming eruption

Considering its large volume, Sumisu's caldera-forming eruption must have overwhelmed the proximal marine environment. Dispersal mechanisms were probably complex, and most details are unknown. With these caveats in mind, we discuss what we consider the three most important dispersal mechanisms (Fig. 11).

Rafts of floating pumice Tangible evidence for pumice rafts, such as accumulations of abraded, rounded clasts of the type illustrated by Manville et al. (1998) and Bryan et al. (2004), was not observed. We nevertheless suggest that such rafts, highly mobile in the open-ocean environment, played an important role in tephra dispersal. As noted earlier, the upper part of the Sumisu edifice was probably an island prior to its caldera-forming eruption, and the eruption column rose into the air. In a process described by Fiske et al. (2001), pumice clasts cooling in the atmosphere would have ingested air as magmatic steam condensed, producing light-weight clasts that floated when they fell into the sea. Hot pyroclastic flows may have traveled over the temporary dry land provided by thick proximal pumice rafts.

Using the August 1883 eruption of Krakatau as an example, the existence of vast fields of floating pumice at Sumisu is a high probability. Floating pumice blanketed wide parts of the Indian Ocean following the Krakatau

eruption (Simkin and Fiske 1983). Three months after the eruption, for example, a merchant vessel 3,000 km west of Krakatau encountered a pumice raft 1,800 km across that locally was sufficiently thick and buoyant to support sailors who jumped onto its surface. More remarkable, 11 months after the eruption (July 1884) masses of pumice washed up on the coast of Zanzibar, >6,000 km from Krakatau. Sumisu's caldera-forming eruption, perhaps two to three times larger in volume than that at Krakatau, probably blanketed widespread parts of the western Pacific with floating pumice.

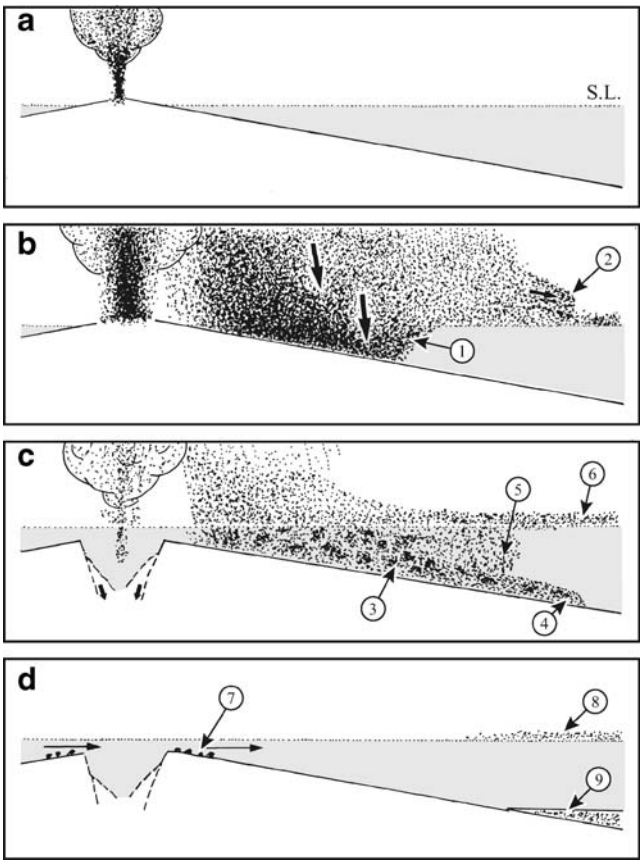

Fig. 11 Cartoon showing four stages of tephra dispersal from the Sumisu caldera-forming eruption, proximal details omitted. Vertical exaggeration X2; sea level (*SL*). **a** Eruption begins on island. **b** Eruption climax. (*1*) Proximal fallback mass, bounded by a seawater exclusion front, temporarily displaces the sea. (*2*) Hot pyroclastic flow travels over raft of floating pumice. **c** Eruption wanes, caldera formed. (*3*) Submarine pumice quenched as seawater gains access to submarine parts of hot, proximal mass (shown schematically by blotchy stipple pattern). (*4*) Pyroclastic density current travels into deeper water. (*5*) Water-column tephra hyperconcentration. (*6*) Floating pumice. **d** Eruption ends. (*7*) Strong ocean currents erode proximal pumice, leaving veneer of dense lithic clasts. (*8*) Floating pumice widely dispersed. (*9*) Deposits of pyroclastic gravity currents mantle distal sea floor

Water-column hyperconcentrations As a process transitional between pumice rafts and pyroclastic gravity currents, we suggest that a large part of the water column, if sufficiently choked with slowly settling tephra, can spread laterally to become an important dispersal mechanism. In Fig. 11c, such a hyperconcentration moves toward the right side of the panel.

Such a scenario could explain the characteristics of the 30-m-thick Quaternary pumice layers cored at ODP Site 788, at the crest of the arc-front ridge 70 km south of Sumisu (Fig. 4), an unlikely place for bottom-hugging gravity currents to be deposited. Nishimura et al. (1991) showed cores from this site to be well sorted, matrix-free, and to contain <1% dense lithic clasts, consistent with an origin involving tephra fallout from water-column hyperconcentrations.

Pyroclastic gravity currents Sumisu's caldera-forming eruption, which began as a subaerial event on a small island, sent an eruption column into the air and delivered hot fallback debris to the proximal marine environment at prodigious rates. Large volumes of this debris entered the sea and remained under water to travel downslope to ODP sites, 70 km distant. But how did this subaerial-submarine transition take place? We suggest that the high density of seawater, as compared with air, temporarily constrained the lateral dispersal of tephra. This resulted in the proximal growth of a thick and rapidly growing mass of hot tephra, a transient feature the upper part of which lay above sea level, and the base of which was depressed to ocean depths of perhaps a few hundred meters. Hot tephra in the submerged part of the mass was initially filled with steam and other magmatic gases (Fig. 11b), an environment that temporarily excluded surrounding seawater. In time, however, the steam condensed (Fig. 11c), seawater entered the mass, and while still below sea level, hot pumices quenched, ingested water, and were transformed from floaters to sinkers. The resulting sludge of water-saturated pumice was then available for downslope transport in pyroclastic gravity currents. Pumice clasts that failed to saturate during this process may have risen toward sea level, accumulating along the base of the pumice raft.

After the eruption (Fig. 11d), Sumisu's caldera rim may have lain at ocean depths of 100 m or less, and parts of it were likely emergent during times of late Pleistocene low stands of sea-level. Strong ocean currents scoured this rim, resedimenting, or removing altogether, much of the syn-caldera pumice deposits originally present. As a result, the thin proximal carpet of dense lithic clasts is the most conspicuous deposit remaining from the caldera-forming eruption.

Conclusions

Sumisu volcano, a large submarine volcano at the front of the Izu-Bonin arc, was the site of a late Pleistocene caldera-forming eruption that introduced ~48–50 km^3 of rhyolite tephra and non-juvenile lithic clasts into the open-ocean environment. Our chief conclusions are:

1) A cluster of small seafloor dacitic and basaltic volcanoes formed at ocean depths of ~1,000 m; these coalesced and grew above sea level to form an island ~200 m high.
2) The caldera-forming eruption resulted in the destruction of most of the island and the surrounding shallow-water parts of the Sumisu edifice. The 8×10 km rim of the present-day caldera lies at ocean depths of 100–400 m.
3) Syn-caldera tephra was dispersed mostly by a combination of sea-surface pumice rafts, hyperconcentrations of slowly settling tephra that drifted laterally in the water column, and pyroclastic gravity currents that traveled tens of kilometers downslope into ocean depths >2 km.
4) Geochemical similarities suggest that the thick pumice deposits encountered at ODP Leg 126 localities, 70–90 km distant, originated at Sumisu volcano. It is likely that Sumisu's caldera-forming eruption was the source of one of these deposits.
5) Post-caldera edifice instability resulted in the failure of a ca 15° sector of Sumisu's eastern caldera rim and the formation of wavy slump structures that disturbed widespread parts of the volcano's surface.

Acknowledgements We are indebted to the captains, operations teams, marine technicians, and crews of the JAMSTEC Research Vessels *Natsushima*, *Kairei*, *Kaiyo*, and *Yokosuka* for their expert help at sea. We thank Hiroshi Kawabata and Naoko Irino for XRF analyses. Adam Klaus and Shoichi Oshima provided bathymetric data. Hideto Yoshida helped us with carbonate analyses. Reviews by Sharon Allen, Peter Kokelaar, and Jocelyn McPhie greatly improved the manuscript. Part of this research was supported by a Grant-in-Aid for Scientific Research (to Y.T.) from the Japan Society for the Promotion of Science (JSPS).

References

Bacon CR (1983) Eruptive history of Mount Mazama and Crater Lake caldera, Cascade Range, USA. J Volcanol Geotherm Res 18:57–115

Bacon CR, Lanphere MA (2006) Eruptive history and geochronology of Mount Mazama and the Crater Lake region, Oregon. Geol Soc Am Bull 118:1331–1359

Bonatti E, Lawrence JR, Hamlyn PR, Breger D (1980) Aragonite from deep sea ultramafic rocks. Geochim Cosmochim Acta 44:1207–1214

Bryan S, Cook A, Evans JP, Colls PW, Wells MG, Lawrence MG, Jell JS, Greig A, Leslie R (2004) Pumice rafting and faunal dispersion during 2001–2002 in the Southwest Pacific: record of a dacitic submarine explosive eruption from Tonga. Earth Planet Sci Lett 227:135–154

Carey S, Sigurdsson H, Mandeville C, Bronto S (2000) Volcanic hazards from pyroclastic flow discharge into the sea: examples from the 1883 eruption of Krakatau, Indonesia. Geol Soc Am Spec Pap 345:1–14

Chappell J, Shackleton NJ (1986) Oxygen isotopes and sea level. Nature 324:137–140

Druitt TH, Bacon CR (1986) Lithic breccia and ignimbrite erupted during the collapse of Crater Lake Caldera, Oregon. J Volcanol Geotherm Res 29:1–32

Druitt TH, Sparks RSJ (1982) A proximal ignimbrite breccia facies on Santorini, Greece. J Volcanol Geotherm Res 13:147–171

Fiske RS, Naka J, Iizasa K, Yuasa M, Klaus A (2001) Submarine silicic caldera at the front of the Izu-Bonin arc, Japan: voluminous seafloor eruptions of rhyolite pumice. Geol Soc Am Bull 113:813–824

Freundt A (2003) Entrance of hot pyroclastic flows into the sea: experimental observations. Bull Volcanol 65:144–164

Gibson HL, Morton RL, Hudak GJ (1999) Submarine volcanic processes, deposits, and environments favorable for the location of volcanic-associated massive sulfide deposits. Rev Econ Geol 8:13–51

Gill JB (1981) Orogenic andesites and plate tectonics. Springer, Berlin Heidelberg New York

Gill JB, Seales C, Thompson P, Hochstaedter AG, Dunlap C (1992) Petrology and geochemistry of Pliocene-Pleistocene volcanic rocks from the Izu arc, Leg 126. In: Taylor B, Fujioka K, Janecek TR, Langmuir C (eds) Proc ODP, Sci Results 126:383–404

Hochstaedter AG, Gill JB, Taylor B, Ishizuka O, Yuasa M, Morita S (2000) Across-arc geochemical trends in the Izu-Bonin arc: constraints on the source composition and mantle melting. J Geophys Res 105B1:495–512

Hudak GJ, Morton RL, Franklin JM, Peterson DM (2003) Morphology, distribution, and estimated eruption volumes for intracaldera tuffs associated with volcanic-hosted massive sulfide deposits in the Archean Sturgeon Lake caldera complex, northwestern Ontario. AGU Geophys Mono 140:345–360

Iwabuchi Y (1999) Sumisu caldera. Jpn Mar Sci Technol Cent J Deep Sea Res 15:83–94 (in Japanese with English abstract)

Keating BH, Helsley CE, Karogodina I (2000) Sonar studies of submarine mass wasting and volcanic structures off Savaii Island, Samoa. Pure Appl Geophys 157:1285–1313

Klaus A, Taylor B, Moore GF, MacKay ME, Brown GR, Okamura Y, Murakami F (1992) Structural and stratigraphic evolution of the Sumisu rift, Izu-Bonin arc. In: Taylor B, Fujioka K, Janecek TR, Langmuir C (eds) Proc ODP, Sci Results 126:555–573

Manville V, White JDL, Houghton BF, Wilson CJN (1998) The saturation behavior of pumice and some sedimentological implications. Sediment Geol 119:5–16

Morishita Y, Matsuhisa Y (1984) Measurement of carbon and oxygen isotope ratios of carbonate reference samples. Bull Geol Surv Japan 35:69–79 (in Japanese with English abstract)

Mueller W, Doucet P, Chartrand F (1994) Archean, deep-marine, volcanic eruptive products associated with the Coniagas massive sulfide deposit, Quebec, Canada. Can J Earth Sci 31:1569–1584

Murakami F, Ishihara T (1985) Submarine calderas discovered in the northern part of Izu-Ogasawara arc. Gekkan Chikyu (Earth Monthly) 106:70–86 (in Japanese)

Nagaoka S, Okino K, Kato S (1991) Landforms of submarine volcanoes in central part of the Izu-Ogasawara arc, by multi-

beam sounding system. Rep Hydrogr Res 27:145–172 (in Japanese with English abstract)

Nishimura A, Marsaglia KM, Rodolfo KS, Colella A, Hiscott RN, Tazaki K, Gill JB, Janecek T, Firth J, Isiminger-Kelso M, Herman Y, Taylor RN, Taylor B, Fujioka K, Leg 126 Scientific Party (1991) Pliocene–Quaternary submarine pumice deposits in the Sumisu rift area, Izu-Bonin arc. In: Fisher RV, Smith GA (eds) Sedimentation in volcanic settings. Soc Sedim Geol Spec Publ 45:201–208

Nishimura A, Rodolfo KS, Koizumi A, Gill J, Fujioka K (1992) Episodic deposition of Pliocene–Pleistocene pumice from the Izu-Bonin arc, Leg 126. In: Taylor B, Fujioka K, Janecek TR, Langmuir C (eds) Proc ODP, Sci Results 126:3–21

Shukuno H, Tamura Y, Tani K, Chang Q, Suzuki T, Fiske RS (2006) Origin of silicic magmas and the compositional gap at Sumisu submarine caldera, Izu-Bonin arc, Japan. J Volcanol Geotherm Res 156:187–216

Siebert L, Simkin T (2002) Volcanoes of the world: an illustrated catalog of Holocene volcanoes and their eruptions. Smithsonian Institution, Global Volcanism Program Digital Information Series, GVP-3 (http://www.volcano.si.edu/world/)

Simkin T, Fiske RS (1983) Krakatau 1883 the volcanic eruption and its effects. Smithsonian Institution Press, Washington, DC

Smith IEM, Stewart RB, Price RC (2003) The petrology of a large intraoceanic silicic eruption: the Sandy Bay Tephra, Kermadec Arc, Southwest Pacific. J Volcanol Geotherm Res 124:173–194

Tamura Y, Tatsumi Y (2002) Remelting of an andesitic crust as a possible origin for rhyolitic magma in oceanic arcs: an example from the Izu-Bonin arc. J Petrol 37:1307–1319

Tamura Y, Tani K, Ishizuka O, Chang Q, Shukuno H, Fiske RS (2005) Are arc basalts dry, wet, or both? Evidence from the Sumisu caldera volcano, Izu-Bonin Arc, Japan. J Petrol 46:1769–1803

Tani K, Kawabata H, Chang Q, Sato K, Tatsumi Y (2005) Quantitative analyses of silicate rock major and trace elements by X-ray fluorescence spectrometer: evaluation of analytical precision and sample preparation. Front Res Earth Evol 2:1–8

Taylor B, Brown G, Fryer P, Gill JB, Hochstaedter AG, Hotta H, Langmuir CH, Leinen M, Nishimura A, Urabe T (1990) ALVIN-SeaBeam studies of the Sumisu rift, Izu-Bonin arc. Earth Planet Sci Lett 100:127–147

Walker GPL (1985) Origin of lithic breccias near ignimbrite source vents. J Volcanol Geotherm Res 25:157–171

Wright IC, Gamble JA, Shane PAR (2003) Submarine, silicic volcanism of the Healy caldera, southern Kermadec arc (SW Pacific): I—Volcanology and eruption mechanisms. Bull Volcanol 65:15–29

Wright IC, Worthington TJ, Gamble JA (2006) New multibeam mapping and geochemistry of the 30°–35° S sector, and overview, of southern Kermadec arc volcanism. J Volcanol Geotherm Res 149:263–296

Yuasa M, Nohara M (1992) Petrologic and geochemical along-arc variations of volcanic rocks on the volcanic front of the Izu-Ogasawara (Bonin) arc. Bull Geol Surv Japan 43:421–456

Yuasa M, Murakami F, Saito E, Watanabe K (1991) Submarine topography of seamounts on the volcanic front of the Izu-Ogasawara (Bonin) arc. Bull Geol Surv Japan 42:703–743